

LECTURE 10

LUMINOSITY FUNCTIONS AND FIELD
GALAXY POPULATION EVOLUTION

L. Tresse

*Istituto di Radioastronomia del CNR, Via Gobetti, 101, I-40129 Bologna
Laboratoire d'Astronomie Spatiale, BP8, F-13376 Marseille Cedex 12*

1. INTRODUCTION

Galaxy redshift surveys are outstanding tools for observational cosmology. Mapping the universe as outlined by galaxies leads to fundamental measurements which refine our knowledge of its structure and evolution. Redshift acquisition has undergone tremendous progress thanks to advances in technology, and redshift surveys appear nowadays as routine. Even though they may look simple at face-value, the strategy of a survey and the galaxy-selection criteria have crucial impacts on the interpretation of results. Since galaxies are directly observable point-like tracers of dark matter halos, they represent only the tip of the iceberg of what drives the evolution of the universe. Hence interpretation of these surveys via model-dependent approaches such as semi-analytical models, N-body simulations provide also fundamental insights into galaxy evolution and formation. Redshift surveys can be analyzed using many different statistical techniques to give measurements of clustering, large-scale structures, velocity fields, luminosity functions, weak-lensing.

In this lecture, I concentrate on one of these measurements, i.e. the galaxy luminosity function (LF) and its evolution. In particular I consider the LF derived from optically magnitude-selected field galaxy redshift surveys. The LF is a fundamental measurement of the statistical properties of the population of galaxies; it is the comoving number density of galaxies as a function of their intrinsic luminosity. The luminosity of a galaxy evolves according to the evolution of its content (see lectures of Charlot and Matteucci), and ac-

ording to its interaction/mass accretion/merging history. Measuring the LF at different cosmic epochs enables us to quantify its changes and to assess the evolution in the galaxy population. Early work on galaxy number counts as a test for evolution has largely been superseded by large redshift surveys which allow the direct determination of the LF from which the observed $N(m)$ and $N(z)$ can be reproduced and better understood. Ultra deep number counts are still used at depths where automatic redshift acquisition is not yet possible (see Ferguson's lecture for an up-to-date review of number counts). I discuss only field galaxies which are selected without regard to their environment or any special properties, hence their study is representative of the global galaxy population. LFs have also been measured from samples which select only either AGN galaxies, or radio galaxies, or $H\alpha$ emitters, or galaxies in clusters, or clusters, etc. These latter measurements determine the evolution of single populations; but the completely different selection means that their connection to the field galaxy population is not straightforward. With large, distant and multi-wavelength surveys of field galaxies, it will be possible to measure the LF for the global population, and for each of these special subsamples, and thus to relate them more easily at different epochs.

The aim of this lecture is to describe the approach to designing state-of-the-art of galaxy surveys and their impact on measurements on LFs. I start by discussing survey strategies, which I consider to be the most important step (Section 2). I continue by describing the data required (Section 3), and then review the different estimators to measure LFs (Section 4). I discuss the LF evolution (Section 5) and I follow by summarizing the status of LF measurements (Section 6). I would like to emphasize that a survey for which one can define and quantify the biases and selection criteria, is more useful in the long term than a survey for which they are not well determined, no matter how pioneering the work is. Indeed comparing data from different surveys is a nightmare, and comparing them to models is even less straightforward. All surveys have different selections, biases and methodologies, and so the interpretation of apparent discrepancies should be done with care before invoking any exotic explanations. The references quoted for the surveys are usually those estimating the LF; references for the series of papers issued from a survey should be found within.

2. SURVEY STRATEGIES

A survey strategy includes choices and constraints at several levels, some of which are described in this section. If not well-defined and well-controlled, poor choices can produce unknown biases toward certain types of galaxy, which will hinder and confuse analysis of the survey.

2.1. From the local to deep universe

One crucial aspect of the preparation of a redshift survey is to find a balance between the sky coverage (i.e. the area of sky in which galaxies are selected for spectroscopic observations), the sampling rate (i.e. the number of spectroscopic targets out of the number of photometric objects within a magnitude range) and reasonable observing times (which depend on the detectors and telescopes used). If these are not handled, it leads to major difficulties to interpret and compare LFs, and even worse for correlation functions or close-pair analysis. Observational strategies are quite different for the local universe ($z < 0.1$) and the distant universe ($z \gg 0.1$).

What matters for the local universe ($z < 0.1$) is the large sky coverage, indeed any single small area is strongly affected by density inhomogeneities. Until recently the way to survey large areas was to use photographic plates of ~ 25 sq. deg field of view. The SDSS ([38]) will be the first large local survey with galaxies selected from CCDs. For local surveys the magnitude limit is about $B \sim 16$, and exposure time required for a spectrum is a few minutes. A full sampling strategy is necessary when aiming to refine the local structures (CfA2 [42], SSRS2 [11]), see da Costa's lecture), but is time consuming (over several years, changes in detectors, strategies lead to disparities within one sample). Meanwhile sparse-sampling strategies have also been adopted (SAPM [35]), or a collection of pencil-beams (KOSS [27]). While these previous surveys observed spectra one by one, wide-field multi-object spectroscopy has been more recently used by Autofib/LDSS [15], LCRS [33], CS [21], and ESP [58] surveys. The ongoing 2dF ([41]) and SDSS use even larger multiplex gain, respectively 2×200 , and 2×320 fibers in one exposure (~ 1 hour). Sampling galaxies $B \simeq 19.5$, these will have a mean depth of $z \simeq 0.1$.

Pushing deeper ($0.2 < z < 1.3$) and with multi-object spectroscopy, redshift surveys (see references in Table 2) are done in pencil beams of few arcmins, with faint magnitude limit ($B < 24$) and long exposure spectra (few hours). The acquisition of several pencil beams is necessary either to cover contiguous patches on the sky or to sample different fields of view over the sky, and several exposures are usually required on the same field. One of the original aim of these surveys was the LFs (and also clustering), indeed studying structures is reliable only with larger areas. Surveys at $1.3 < z < 2.7$ require detectors sensitive in the infrared since no strong spectral features are observed in the optical wavelength range. This cosmic epoch will very soon be surveyed by 8m class telescope (see lecture of Le Fèvre). For higher redshifts ($z < 4 - 5$), the existing redshift survey ([54]) has selected only a certain type of galaxies (the Lyman break population). Systematic redshift surveys in this range will be also conducted with 8m telescopes. The universe at $z > 5$ is still an unknown regime, but some models suggest that there is a population of galaxies already formed. If such a population exists, the distances between galaxies (or any subgalactic mass undergoing star formation) will be smaller, and the apparent size of galaxies larger, leading to very crowded fields. Thus methods such

as Integral Field Unit may be chosen rather than traditional MOS, and are under studies in particular for the Next Generation Space Telescope as well as Micro-Mirror or Micro-Shutter Arrays MOS (see “NGST - Science Drivers & Technological Challenges”, 34th Liege International Astrophysics Colloquium, June 1998, ESA Publications).

2.2. MOS modes

Each survey using multi-object spectroscopy (MOS) has biases introduced by the constraints inherent to the particular MOS mode used. For instance when using fiber multiplex, a set of fibers is placed on objects while another set is placed on sky. Since the sky spectrum is measured through different fibres than the galaxies, the throughput and spectral response will be different and this can lead to poor sky subtraction, especially for faint galaxies whose flux is a small fraction of sky. Also fibres typically cannot be placed closer than $20''$ from one another, which leads to a bias against close pairs of galaxies unless fields are observed several times. Using slit multiplex, a slit is placed on an object including sky on both side, and can include close objects. However, while the output spectrum from a set of fibers is arbitrarily reorganized on the CCD, it is not the case with slits for which the spectrum is dispersed on both sides of the aperture location on the CCD. No other objects can be observed in the CCD area covered by the spectrum within one observation. This produces non-uniform selection patterns in the dispersion direction, i.e. some areas are more sampled than others. Depending on the number of observations (or the sampling rate aimed), these effects can be reduced but at the cost of the volume surveyed within a certain allocated time. Basically the number of possible slits/fibers to be positioned on galaxies is function of galaxy density (related to the magnitude range sampled) and the number of observations on the same sky area. Thus to get a 100% sampling is somewhat time consuming. A compromise has to be reached between the full use of the multiplex gain and the uniformity in (x, y) of the galaxies selected. There are even more subtle biases with both MOS modes. The quantification of such effects is not straightforward; simulations are helpful to measure them, and take them into account in statistical analysis.

2.3. A priori selections

One common pre-selection for objects to be observed in spectroscopy mode is the galaxy/star separation. Depending on the survey magnitude range, the number of stars can be so high that it is necessary to do this pre-selection to avoid spending most of the time observing stars. For instance in the SAPM magnitude range ($15 < b_J < 17$, see [36]), stars are $\sim 95\%$ of the objects! However the galaxy/star separation techniques are not 100% reliable, for example such pre-selection is likely to exclude compact galaxies (in the APM it has been estimated at 5%, [40]). For deep surveys this is less crucial. For instance in the

CFRS magnitude range ($17 < I < 22$) no-preselection was done, and depending on the field galactic latitudes, from 10 to 30% of objects were stars of mostly M and K types. Another pre-selection is to choose the objects by eye. In these cases, nice objects, close objects, peculiar objects will tend to be selected introducing a non-controlled bias.

2.4. Photometric choices

Objects in redshift surveys were usually selected from one pass-band of wavelengths, and this leads to a preference for a certain type of galaxy. Since the detectors were the most sensitive in the blue, the first redshift surveys selected galaxies from their flux received around 4400 \AA . Thus the observed rest-frame luminosity spans the ultraviolet wavelengths ($4400/(1+z)$), and this comes down to select galaxies mostly on their current star-formation activity. The UV emission is known to be strongly dust extinguished (for instance the flux is reduced by a factor $2 - 3$ for galaxies at $z \sim 0.2$, [55]), and is usually much fainter than the optical for spiral and elliptical galaxies. Hence galaxies become difficult to detect especially at $z > 0.5$, and those observed are likely to be only the strong star-forming galaxy population. Recent deep surveys selected galaxies from their red or infrared observed flux. This enables us to observe galaxies at $z > 0.5$ more easily since the spanned rest-frame light lies in the optical. This selection is closer to the galaxy mass regardless the current star-forming activity, and so the observed population is more representative of the total galaxy population.

Single pass-band surveys select galaxy populations which are never fully homogeneous from one cosmic epoch to another. To quantify the fraction and type of galaxies over or under-observed is not straightforward, and requires multi-color selected samples. This leads to LF measurements at various epochs which are derived from different observed galaxy populations, and it has to be handled with care when studying evolution of LF. Color-selected samples searching for the Lyman break (or UV dropout), are recently used for galaxies at $z > 3$, but select only the galaxy population for which this break is detectable ([54]). With large on-going multi-wavelength surveys, several samples of multi-color selection should be more homogeneous.

Another important selection criterion is the way the magnitudes are measured, and thus how the objects are selected. Photographic magnitudes are more difficult to calibrate than CCD magnitudes, due to the non-linearity and saturation occurring in photographic plates; these effects are non trivial to correct, even when calibrating with a sub-set of CCD magnitudes. To be complete down to a certain magnitude in a single band, the best is to use total magnitudes. However since the outer part of galaxies is usually below the threshold detection (i.e. a small fraction of the surface brightness of the night sky), in practice total magnitudes are not measured directly and are retrieved from aperture or isophotal magnitudes. Recovering for the lost flux can be subject to systematic errors and ultimately requires knowledge of the surface brightness

(SB) profile, and thus most surveys quote a photometric completeness based on their choice of flux measurement.

Actually catalogues are limited by an apparent magnitude, a SB and a size. The usual truncation of a catalogue to a magnitude limit results in biases in SB and size which add complexity when comparing surveys, or when recovering the galaxy densities (see for instance [46], [24] and references within). Isophotal magnitudes include a varying fraction of the total flux due the $(1+z)^{-4}$ SB dimming effect, and different galaxy SB profiles; to be close to the total magnitude the adopted isophote limit must correspond to about 6 magnitudes fainter than the total magnitude (for instance if $m_{tot} = 22$, $SB = 28$ mag arcsec $^{-2}$, [31]). Petrosian magnitudes integrate the flux within a radius determined by the ratio of the mean SB within radius r to the local surface brightness at r ([45]). Aperture magnitudes can be used with an empirical fit to the galaxy light-growth curve to integrate the flux within an area close to the total flux emitting area; the required galaxy image center is usually recovered from an isophotal measurement. For instance Kron aperture magnitudes ([28]) integrate the flux within a radius which is a multiple of the first moment radius (r_1) of the intensity-weighted radial profile ($r_{Kron} \simeq 2r_1$). The integrated flux with these methods reliably reaches 90-95% of the total flux. Some complications occur when galaxy images overlap, or when strong emitting regions in the outer disk can be taken mistaken for another object.

To be complete down to a certain color, the light must be integrated from the same emitting area of a galaxy. This can be done within a fixed aperture and considering the same center for different pass-band images, or using an isophotal area defined from the sum of these images. Magnitudes that are close to total magnitudes are the most attractive to use in defining a sample, because it is then easy to select well-defined sub-samples as, for instance, a fixed aperture magnitude sample for work on a color-selected sample. Starting from a fixed aperture-selected sample it is not possible to generate a sample complete to a given total magnitude. Total magnitudes are also attractive to study low-surface brightness and intrinsically faint galaxies.

2.5. Spectroscopic choices

The choice of the spectral resolution ($\Delta\lambda/\lambda$) has an impact on the success rate for measuring a z . For instance, if the observed z range (related to the magnitude range) is large, a low-resolution allows to observe a large wavelength range, and increases the chances to observe an emission line as the common [O II], and/or the Balmer break. On the contrary, a high-resolution is better to work out the spectral properties of galaxies, including H δ , H β , d_{4000} , H α , [O II] measurements for star-formation rate, metallicity and spectral classification. With new infrared detectors to observe galaxies at $1 < z < 3$, a high resolution is better to correct for the strong OH sky emission and assure the z measurement. Another point is that it is preferable to span wavelengths that are within the filter-band of selection for galaxies so that the spectroscopy com-

pleteness correlates with the photometric observations. To measure a z , flux calibration is not necessary. However again if the spectral properties are studied at several z , it is better to obtain calibrated spectra. Spectro-photometric calibration also enables us to correct for aperture light losses. Several exposures are required to filter out the cosmics. A signal-to-noise of 10 or more is required if one wants to avoid a bias against spectra with weak features. The choice of the aperture has also its importance in the success rate for finding a redshift; slits of $\sim 1.5''$ are usually used for deep surveys. The success rates for redshift surveys can reach levels of $\sim 90\%$, and are usually function of the magnitude; at the faint limit of a survey incompleteness can be very large!

3. BASIC DATA REQUIRED TO MEASURE LF

The basic data needed for each targeted object of a survey are the redshift z , the relative magnitude m , and the galaxy type. It is important that each step is well-defined so that the redshift completeness function and the uncertainties in the absolute magnitude determination can be established for the survey.

3.1. Redshifts

The method to measure z from a sky-subtracted optical spectrum is to identify a set of spectral features which have the same ($\lambda_{obs}/\lambda_{rest} = 1+z$). Note that $\lambda_{rest} > 2000\text{\AA}$ is measured in the air, while $\lambda_{rest} < 2000\text{\AA}$ in the vacuum; in this last case $(1+z)$ has to be multiplied by the refractive index of air ($n = 1.0029$). The reliability of z is correlated to the number of features and their signal-to-noise; for instance a single strong emission line is not sufficient to determine securely a z , also for a set of several weak features (for these cases, colors may be helpful to secure z , see below). The simplest way to measure z is to fit individual lines, and/or to cross-correlate with template spectra. Now that thousands of spectra are taken by night, fully automatic measurements of z are necessary; hence supplementary procedures have been developed using for instance Principal Component Analysis (PCA) techniques (see e.g. [9]). The difficult task of such automation is to account for all possible situations as for instance the diversity of spectra (from extremely blue to red spectra, from QSO to stellar spectra, from featureless spectra to very reddened spectra), the problems in the spectra (bad sky subtraction, etc.). Such things could be easily judged by eye, but with the large on-going and future surveys it is impractical to look at them one by one.

In the optical window $[4000-9000]\text{\AA}$, the strongest features are $[\text{O II}] \lambda 3727$, the Balmer break at 4000\AA , $\text{H}\beta$, $[\text{O III}] \lambda\lambda 4959, 5007$, $\text{H}\alpha$, $[\text{N II}] \lambda\lambda 6548, 6583$, $[\text{S II}] \lambda\lambda 6718, 6731$, and followed by $\text{H}\gamma$, $\text{H}\delta$, CaH , CaK . With $[\text{O II}]$ in the optical, one can determine z until 1.4 about, then no strong features appear in the optical until $z \sim 2.2$ where $\text{Ly}\alpha$ (1215\AA) can be observed. To cover the missing region, detectors sensitive in the near infrared window $[0.9-1.5]\mu\text{m}$ are

required to still observe at least [O II].

In principle, measured redshifts must be transformed from the Earth to the Sun system (heliocentric z) then to the galactic center (galactocentric z). This represents about 300 km s^{-1} or 0.001 in z . In the very nearby universe ($z < 0.03$), peculiar velocities of galaxies are not negligible compare to the Hubble radial velocity flow of $300\text{--}500 \text{ km s}^{-1}$, i.e. when $v_{\text{radial}} < 10000 \text{ km s}^{-1}$. The accuracy usually aimed is better than 0.001 in z . Another point is that absorption lines do not always give the same z as emission lines (velocities can differ by up to $\sim 500 \text{ km s}^{-1}$). This is usually explained by the fact that emission lines originate in different regions than absorption lines, and that this effect is enhanced when galaxies are seen edge-on.

Another way to determine redshifts is to use the colors of a galaxy, which corresponds to using an extremely poor resolution spectrum since a color is the integrated flux over several wavelengths. Thus they are inferred from the spectrum shape, and mainly from the location of the discontinuities in the continuum (Balmer, Lyman breaks). These redshifts are called photometric redshifts; they rely strongly on the knowledge of the spectral energy distribution and its evolution for any type of galaxies, and cannot give precise measurement. To avoid catastrophic identifications, UV and IR colors are absolutely essential, and the error in z is reduced to ~ 0.03 in z ([8]). They were first used when acquisition of spectra was extremely time consuming, and have recently come back to fashion to estimate redshifts of very distant galaxies as seen in the Hubble Deep Field, where spectroscopy requires at least 8m telescopes. They are particularly useful in the presently region at $z = 1.4 - 2.2$, where there are no strong optical features. Actually they are a useful technique to estimate the z of a galaxy, and thus to select the window (optical or infrared, thus the instrument) in which prominent features are likely to be seen in spectroscopy.

If no redshift can be measured for a galaxy, then it is part of the redshift incompleteness of the survey. It is important to quantify this as a function of magnitude, and to understand where it may come from (only low SB galaxies?, only high- z galaxies?, problem with the slit/fiber, etc.).

3.2. Absolute magnitudes

Magnitudes are determined in a well-defined pass-band such as B, V, R, I , or K . Denoting the band as j , the absolute magnitude is $M_j = m_j - DM - k_j - A_j$ where DM is the modulus distance depending only on the world model chosen (H_0 and q_0), m the apparent magnitude, k the correction necessary to express all magnitudes in the same rest-frame filter band, and A the galactic extinction. This is the classical way to measure absolute magnitudes in redshift surveys, which minimizes model-dependent inputs. Then when comparing with models, these magnitudes can be corrected, as wished, for the predicted luminosity evolution of a certain type of galaxy at z in the same rest-frame band, and for reddening produced by the dust extinction intrinsic at each galaxy. However accounting only for the k -correction, the measure of M is already

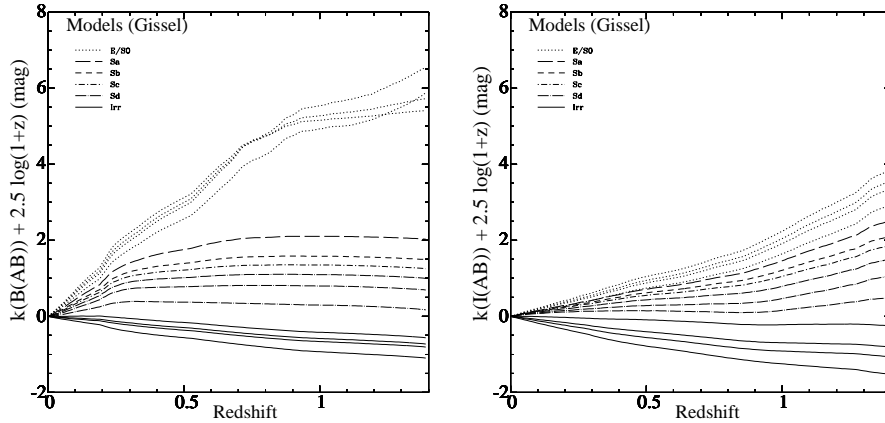


Fig. 1. — k -corrections minus $2.5 \log(1+z)$ in B_{AB} (left) and in I_{AB} (right) using Gissel types (see [5]) from E (top lines) to Irr (bottom lines) spectral types.

model-dependent (assuming a world model). Depending on the galaxy type the model-dependent term of k -corrections spans ~ 4 magnitudes in B, and ~ 2 magnitudes in I at $z=1$ (see Fig. 1). Thus it is crucial to determine accurately the galaxy type. The best is to use (multi-)color information; the spectral continuum may also be used but sometimes cannot accurately constrain a type depending on the rest-frame wavelength range observed and the spectral resolution. Morphological information has also been used for local galaxies, but because of the miss- or non-classification of certain galaxies it is not as reliable as colors. One way to minimize the k -correction is to use the relative magnitude which spans the rest-frame band in which absolute magnitudes are expressed. For instance, for galaxies around $z \sim 0.2$, ~ 0.9 and ~ 2.7 , respectively m_V , m_I and m_H spans the rest-frame B band, so the k -correction is small, and at these exact z , the model-dependent term of the k -correction is null. Also k -correction can be directly measured from a flux-calibrated spectrum if the observed wavelength range includes both the observed- and rest-frame bands; but this measure depends on the quality of the calibrated spectra. The proper determination of k -corrections has an impact on the accuracy of M and on the measure of the observable volume of a galaxy used in the LF estimators.

4. ESTIMATORS FOR THE LUMINOSITY FUNCTION

Several methods have been developed and generalized to estimate the comoving number density as a function of luminosity, i.e. the *luminosity function* (LF) $\phi(L)$ (or $\phi(M)$) expressed as a number of galaxies per Jansky (or per magnitude) per cubic megaparsec. Table 1 summarizes the estimators that have

Table I. — Table summarizing different methods to estimate the LF (see text) with in column (1) the estimator name, (2) the assumption or not of a parametric function for the LF, (3) the assumption on $\rho(\mathbf{r})$, (4) the output for the LF, (5) the references which are not exhaustive for a question of space (fully detailed ones are given in [2] and [57]).

| (1) | (2) | (3) | (4) | (5) |
|-------------|-----|----------------------|-------------------|------------------|
| V_{max} | no | uniform ¹ | ϕ, L, α | [51], [17], [13] |
| C^- | no | spherical | ϕ, L, α | [30], [7] |
| ϕ/Φ | no | none | L, α | [56], [26], [12] |
| STY | yes | none | L, α | [49] |
| SWML | no | none | L, α | [16], [22], [53] |

¹ In practice, the density is assumed constant in the range of redshifts in which the LF is estimated.

been used; for a comprehensive review on estimators and history, see [57] and references within. These estimators usually assume that the luminosity L is uncorrelated with spatial location \mathbf{r} , so that the comoving number density at a distance \mathbf{r} as a function of luminosity can be written as $\Phi(L, \mathbf{r}) = (\rho(\mathbf{r})/\overline{\rho(\mathbf{r})}) \phi(L)$ where $\rho(\mathbf{r})$ is the galaxy *density function* (DF). The assumed separability of LF and DF means for instance that the LF is supposed to be the same in clusters and in the field which have different DF. This assumption led to estimators which are independent of the spatial galaxy distribution even though it is inhomogeneous on small and large scales. I emphasize now that correlations *are* observed between galaxy properties and the neighborhood density. The separability of L and \mathbf{r} remains if the LF is calculated at a certain cosmic epoch, with estimators extended to be applied as a function of redshift. Hence estimators assume that $\phi(L)$ is uncorrelated to (x, y) , and changes only a little within a small range of redshifts.

Estimators for the LF differ mainly in how they evaluate the probability of observing a galaxy with a luminosity L and type i in a given volume of the universe. The volume is usually defined by the low and high apparent magnitude limits of a survey, and by the redshift bin analysed giving a minimal and maximal redshift. Actually the SB and size limits should also be taken into account if well-defined samples in SB and size are used. These estimators rely on the Bayes' theorem which in this case says that, in the absence of prior information, the most likely LF given the observations is the one which would most often reproduce the observed distribution of galaxy luminosities in a series of equally likely realizations. Thus we maximize the joint probability for the observables. Usually this is done by maximizing the likelihood function, defined as $\log_e \mathcal{L} = \log_e \prod_i p(L_i) = \sum_i p(L_i)$.

Briefly, V_{max} estimators are simply based on the inverse sum of the maximum

observable comoving volumes of each galaxy. They assume a uniform density and thus are affected by clustering in the galaxy distribution. STY, SWML and ϕ/Φ estimators cancel out in the calculations the density, so they are clustering insensitive methods. The C^- method assumes a spherical density, i.e. the LF has the same shape at any (x, y) , so is ideal for pencil-beam rather than large-angle surveys. We note that all estimators can account for the completeness function.

Local surveys ($\bar{z} \sim 0.05$) are strongly affected by the density fluctuations of the Virgo and Coma clusters in the North hemisphere, and by a local void in the South. For example, Willmer ([57]) compares different estimates of the LF, using the CfA1 redshift survey, and find large discrepancies caused by the Virgo cluster which dominates this survey. For slightly deeper local surveys ($\bar{z} \sim 0.1$), these discrepancies are much reduced. The V_{max} density-dependent estimates give higher faint-end shape when the observed area is cluster dominated, but if the area is large and deep enough, the effects of clusters and voids are counter-balanced and the V_{max} estimate is similar to clustering insensitive estimates as seen in the 2dF ([41]). Distant surveys ($z \gg 0.1$) which sample galaxies in pencil-beam fields of view do not suffer from these local inhomogeneities, but their line of sight through cosmic epochs also crosses structures and voids. Observing several pencil-beams over the sky smoothes this out, and discrepancies between estimates are then small (usually within Poisson error bars).

Even though methods do not assume a parametric function for $\phi(L)$ (save the STY method), the shape of LFs are usually fitted with a Schechter function, i.e. $\phi(L)dL = \phi^*(L/L^*)^\alpha \exp(-L/L^*)d(L/L^*)$, where L^* represents a characteristic luminosity above which the density of more luminous galaxies decreases exponentially, α is the slope of the LF at fainter luminosities (called the faint-end slope), and ϕ^* is the number density of galaxies at L^* (called the normalization). In practice the number densities per magnitude are fitted, i.e. $\phi(M)dM = 0.4 \log_e(10) \phi^* (10^{-0.4(M-M^*)})^{(\alpha+1)} \exp(-10^{0.4(M^*-M)})dM$. Thus we say the slope is steep, flat or negative respectively when $(\alpha + 1) < 0, = 0$ or > 0 . The three Schechter parameters are highly correlated, and thus redshift surveys which sample a large range of luminosities are likely to give the best results for the LF estimation. It is of course a challenge to achieve this at any redshift. The mean galaxy density and mean luminosity density in a comoving volume are respectively $\int \phi(L)dL = \phi^* \Gamma(\alpha+1)$ and $\int L\phi(L)dL = \phi^* L^* \Gamma(\alpha+2)$. The slope is measured $\alpha < -1$; thus for a non-diverging density the LF must have a cut-off at faint L . This cut-off has not yet been observed even in the deepest local survey (ESP). Since the slope is also measured > -2 , the numerous faint L galaxies contribute little to the total luminosity density.

Recently, it appears that the Schechter function is not a good fit to the overall LF over a wide luminosity range ([37], [52], [58]). A modified Schechter function has been used as follows: $\phi(L)dL = \phi^*(L/L^*)^\alpha \exp(-L/L^*) [1 + (L/L_t^*)^\beta] d(L/L^*)$, where L_t is the luminosity at the transition between the two power-laws. This second power-law is introduced to fit the overall LF from

all galaxies, and in particular to allow the fit to steepen at the faint luminosities. The standard Schechter function does not reproduce the up-turn at the faint-end since most weight in the fits comes from galaxies near M^* .

However if a Schechter function fit is done for each individual galaxy type, and a final overall fit constructed from the sum of them, this modified Schechter function is not necessary, since this sum provides the necessary degrees of freedom to allow a faint-end steepening. In fact, various types of galaxies have very different LF; the late types have a very steep slope with a faint M^* , while early types have a negative slope with a luminous M^* . So the overall LF should always be calculated as the sum of each individual population LF, i.e. $\phi(L, \mathbf{r}) = \sum_{sp} \phi_{sp}(L) \rho_{sp}(\mathbf{r}) / \overline{\rho_{sp}(\mathbf{r})}$ where sp refers to a sub-population. These sub-populations can be defined for instance by colors, surface brightness, morphological parameters (morphology types, bulge/disk ratios, asymmetry/symmetry, sizes, lumpiness degrees), spectral parameters (PCA types, line EWs, SED types), nucleus activity, star-formation rates, their environment, etc. For instance, the overall LFs of the preliminary 2dF ([18]) and of the LCRS ([4]) are well fitted over the whole luminosity range in summing the Schechter function fits of each individual PCA spectral type, especially at the faint end ($M(b_j) - 5 \log h > -16$) where the data show a genuine up-turn as in the ESP LF. On the contrary, a Schechter function fit for all galaxies does not correctly reproduce the faint-end slope.

In addition, estimating the LF as the sum of type-dependant LFs avoids the bad assumption that all galaxies are clustered in the same way. Measuring the LFs independently is the same as assuming the separability of L and \mathbf{r} within each individual population. However it does not solve the problem if an individual LF depends on density, as hinted by the results in the LCRS ([4]). They find that the faint-end slope steepens with local density for early-type galaxies from $\alpha = -0.4 \pm 0.07$ in high-density regions to 0.19 ± 0.07 in low-density regions. The strength of such effects is likely to depend on the classifier chosen to define the sub-populations.

The last point is that methods which do not make any assumption about the shape of DF (ϕ/Φ , STY and SWML estimators), recover only the shape of the LF (i.e. α and M^*), and so must normalize the LF in an independent manner usually related to an independent maximum-likelihood estimator. Step-wise estimators calculate the normalization in each magnitude bins. It is clear that the faint-end LF reached by a survey is more uncertain due to the small volume surveyed, and so is more subject to density inhomogeneities.

5. EVOLUTION OF LUMINOSITY FUNCTIONS

A survey with a large baseline in redshift allows the estimation of the LF at different epochs, and hence allows the detection of evolution. This requires observing enough galaxies per bin of absolute magnitudes in each redshift bin. Although number count studies suggested evolution in the field galaxy pop-

ulation, it was controversial ([29], [14]) and only recently has it been clearly detected observationally (CFRS, LDSS, CNOC2). Any changes in the LF with redshift suggest evolution, but care must be taken to account for incompletenesses and biases, and the significance of any changes must be compared to the estimated uncertainties. *Any theoretical interpretation of luminosity functions depends very critically on an understanding of what is being measured and how it is measured.* Parameterizing the LF with a Schechter function adds complexity, since the three parameters (α , L^* , ϕ^*) are strongly correlated. This makes it difficult to disentangle evolution in density and/or in luminosity. Moreover if pure density evolution is detected, it is indistinguishable from density variations caused by large-scale structure; to infer evolution we must assume that the universe is homogeneous on very large scales (see [53]).

Another critical point is that galaxy populations evolve differently, and averaging over all galaxies can mask the evolution of each individual population. As seen in the previous Section, sub-populations have very different LF. The various possible classifiers are certainly related through star-formation history and environmental effects, and using several classifiers will allow us to refine what physically drives the evolution. Only with large and deep surveys evolution can be quantified for different galaxy populations. Moreover selecting galaxies from a single pass-band means that the set of observed galaxies varies with redshift, and can mimic an evolutionary trend. Indeed any particular selection criteria will favour a particular galaxy population. Deep multi-color redshift surveys will be better to quantify which set of galaxies is visible at different redshifts. Surface brightness functions are also needed to quantify which galaxies may be missed because of a low (or high) surface brightness or included due to an enhancement of star formation. Studies of low surface-brightness galaxies show that they are numerous even though they are not a major contributor to the total luminosity density (see for instance [47], [52], [37]).

Extreme care about the methodologies used should be taken when comparing faint-end slope from different surveys; a discrepancy can be mistaken for evolution. The best way to test for evolution is to look within the same survey and use the same estimators for the comparison, to avoid the possible biases discussed earlier in this lecture. This point is even more important for LF measured for a particular type of galaxies, since any classification will be subject to the precise definition of the classifier which may vary from a survey to another one, and to systematic variations in the classifier as a function of redshift. However to link local surveys to distant ones, we always have to rely on comparisons between different surveys. Hence the importance of well-defined surveys.

6. STATUS

For 20 years redshift surveys have taken advantage of fast advances in technology and instrumentation to become larger and deeper. In the last few years, the

study of galaxy evolution has undergone quite a revolution, and is still moving fast. This has been possible thanks to the development of multi-object spectroscopy, and large sensitive detectors on telescopes with good seeing. It has led to a much clearer picture. The qualitative theoretical picture was already in place, but this has now been refined and quantified by the observational constraints from recent redshift surveys. Accurate measurements were crucial to reach the stage where now we can definitely pick the most likely explanations of galaxy evolution and rule out others that flourished earlier on. For the first time, we can trace observationally the global history of galaxy luminosity density up to redshifts of $z \sim 5$ ([39]). The on-going and future redshift surveys should represent a major step towards obtaining a detailed and refined picture of this history. As we saw, to constrain better what drives evolution and how galaxies form, we need to classify galaxies consistently in each redshift bin. We also need to go deep and far, thus large and deep well-defined redshift surveys are required. Table 2 gives the references of papers which estimate LFs, and Figure 2 displays some of them. Below I give a non-exhaustive overview of the current status of LFs.

6.1. Local LFs

The local LF still presents questions for debate. Indeed the discrepancies between various estimates are not yet fully explained. However several come from the methodologies and selection criteria used, so that it is not straightforward to compare the surveys. A major issue has been the normalization of the local LFs. The latest overall LFs at $\bar{z} \sim 0.1$ of blue-selected surveys (ESP, CS, 2dFs, AF) are about consistent with a fairly high normalization and positive faint-end slope. The LCRS differs for reasons that are still uncertain, probably due to surface brightness cuts and/or the selection of galaxies in the red. At larger depths $\bar{z} \sim 0.3$, the ESS, AF/LDSS-b agree also with an high normalization. However for less deep surveys $\bar{z} \leq 0.05$, large discrepancies (up to 50%) in the normalization estimate are found between SSRS2, CfA2, SAPM and Durham/UKST surveys. Multitude of explanations have been given in the literature, however none has been fully convincing just because it invokes possible biases in each surveys that have not been fully quantified yet, while others invoke a local under-density in the southern hemisphere and/or a rapid evolution.

The status for local LF estimates can be summarized as follows:

- (a) At $\bar{z} < 0.1$, significant discrepancies are found between different surveys; the on-going 2dF and SDSS surveys should give more insights to this problem.
- (b) The LF of blue, strongly star-forming, late-type and/or irregulars has a steep faint-end slope ($\alpha < -1$), and faint M^* .
- (c) The LF of red, early-type or E/S0 has a negative slope ($\alpha > -1$).
- (d) The LF of intermediate-type, spirals has a flat slope ($\alpha \simeq 0$).
- (e) A faint end cut-off has been yet not observed at $M(b_j) - 5 \log h = -12.4$.
- (f) LF of galaxies selected in the optical are steeper than those for a infrared

Table II. — Table summarizing published LF analysis from optical-selected redshift surveys (at the end of year 1998). References give details on LFs by type of galaxies. Survey annotated by † are described in proceedings, so are preliminary results. N_{gal} lists the number of galaxy redshifts used in the overall LF estimate (usually α , and M^*), and may differ from the total number of galaxies in the survey itself). Selection is the filter in which galaxies have been selected. c is for CCD mags, and p for photographic mags (even though some plate photometry has been re-calibrated later on with some CCD data). M_{ref} is the pass-band in which LF parameters have been measured ($h = H_0/100$).

| Survey | Selection | $\langle z \rangle$ | N_{gal} | M_{ref} | $M_{ref}^* - 5 \log_{10} h$ | α | $\phi^* \times 10^3 / h^{-3}$ (Mpc^{-3}) | Refs. |
|-----------|----------------------------------|---------------------|-----------|-----------|-----------------------------|------------------|--|-----------|
| CfA2 | $Z \leq 15.5$, p | 0.02 | 9063 | Z | -18.75 ± 0.30 | -1.00 ± 0.2 | 40 ± 10 | [42] |
| CfA2-N | | | 6312 | | -18.67 | -1.03 | 50 ± 20 | [42] |
| CfA2-S | | | 2751 | | -18.93 | -0.89 | 20 ± 10 | [42] |
| SSRS2 | $B(0) \leq 15.5$, p | 0.02 | 2919 | B(0) | -19.50 ± 0.8 | -1.2 ± 0.7 | 15 ± 3 | [11] |
| | $B_{26} \leq 15.5$, p | 0.02 | 3288 | B_{26} | -19.45 ± 0.08 | -1.16 ± 0.07 | 10.9 ± 3 | [43] |
| | $B_{26} \leq 15.5$, p | 0.02 | 5036 | B_{26} | -19.43 ± 0.06 | -1.12 ± 0.05 | 12.8 ± 2 | [44] |
| KOSS | $F_{KOS} \leq 16$, p | 0.04 | 229 | F_{KOS} | -21.07 ± 0.3 | -1.04 ± 0.30 | 15.4 ± 4.9 | [16],[27] |
| DARS | $11.5 \leq b_J \leq 17$, p | 0.04 | 291 | b_J | -19.56 ± 0.2 | -1.04 ± 0.25 | 8.3 ± 1.7 | [16] |
| SAPM | $15 \leq b_J \leq 17.15$, p | 0.05 | 1658 | b_J | -19.50 ± 0.13 | -0.97 ± 0.15 | 14 ± 1.7 | [35] |
| D/UKST | $b_J \leq 17$, p | 0.05 | 2055 | b_J | -19.68 ± 0.08 | -1.04 ± 0.08 | 17 ± 3 | [48] |
| CS | $R_{KC} \leq 16.13$, p | 0.08 | 1695 | R_{KC} | -20.73 ± 0.18 | -1.17 ± 0.19 | 25 ± 6.1 | [21] |
| LCRS | $15 \leq r_g \leq 17.7$, p | 0.1 | 18678 | r_g | -20.29 ± 0.02 | -0.70 ± 0.05 | 19 ± 1 | [33] |
| ESP | $b_J \leq 19.4$, p | 0.1 | 3342 | b_J | -19.61 ± 0.07 | -1.22 ± 0.07 | 20 ± 4 | [58] |
| 2dF† | $b_J \leq 20$, p | 0.1 | 8182 | b_J | -19.54 | -1.166 | 18.3 | [41] |
| AF | $17 \leq b_J \leq 22$, p | 0.15 | 1026 | b_J | -19.20 ± 0.3 | -1.09 ± 0.1 | 26 ± 8 | [15],[22] |
| ESS† | $R_{KC} \leq 20.5$, c | 0.3 | 327 | R_{KC} | -21.15 ± 0.19 | -1.23 ± 0.13 | 20.3 ± 8 | [19] |
| CNOC2† | $R \leq 21.5$, c | 0.3 | 2075 | B_{AB} | -19.43 ± 0.08 | -0.82 ± 0.08 | ~ 10 | [34],[6] |
| AF/LDSS | $17 \leq b_J \leq 24$, p | 0.4 | 1405 | b_J | | | | [15],[22] |
| AF/LDSS-a | $z = [0.02 - 0.15]$ | | 588 | | -19.30 ± 0.13 | -1.16 ± 0.05 | 24.5 ± 3 | |
| AF/LDSS-b | $z = [0.15 - 0.35]$ | | 665 | | -19.65 ± 0.11 | -1.4 ± 0.11 | 14.8 ± 3 | |
| AF/LDSS-c | $z = [0.35 - 0.75]$ | | 152 | | -19.38 ± 0.26 | -1.45 ± 0.17 | 35.5 ± 25 | |
| CFRS | $17.5 \leq I_{AB} \leq 22.5$, c | 0.56 | 591 | B_{AB} | -19.68 ± 0.15 | -0.89 ± 0.10 | 32.8 ± 4 | [32] |
| CFRS-1 | $z = [0.2 - 0.5]$ | | 208 | | -19.53 | -1.03 | 27.2 | |
| CFRS-2 | $z = [0.5 - 0.75]$ | | 248 | | -19.32 | -0.50 | 62.4 | |
| CFRS-3 | $z = [0.75 - 1.0]$ | | 180 | | -19.73 | -1.28 | 54.4 | |

selection, certainly due to different population sampled.

(g) Late-type galaxy populations are fainter than early-type ones, and more numerous at the faint luminosities.

(h) An up-turn at $M(b_j) - 5 \log h < -16$ is genuinely detected, and is generally related to the low-SB galaxies undergoing significant star formation.

(i) Very late-type galaxies are less clustered than early-type ones. The strength of the dependency of the LF with the density for a single type remains to be defined, however early-type LF seems the most affected.

These near-UV and blue rest-frame selected LF shapes reflect the dominant processes in each type of galaxy at low redshifts. Massive galaxies are not dominated by star bursts, while it is for the faint galaxy population. Since blue selection is related to the number of ionizing stars, a steep slope is expected for actively star-forming galaxies dominated by short-time scale evolution (see e.g.

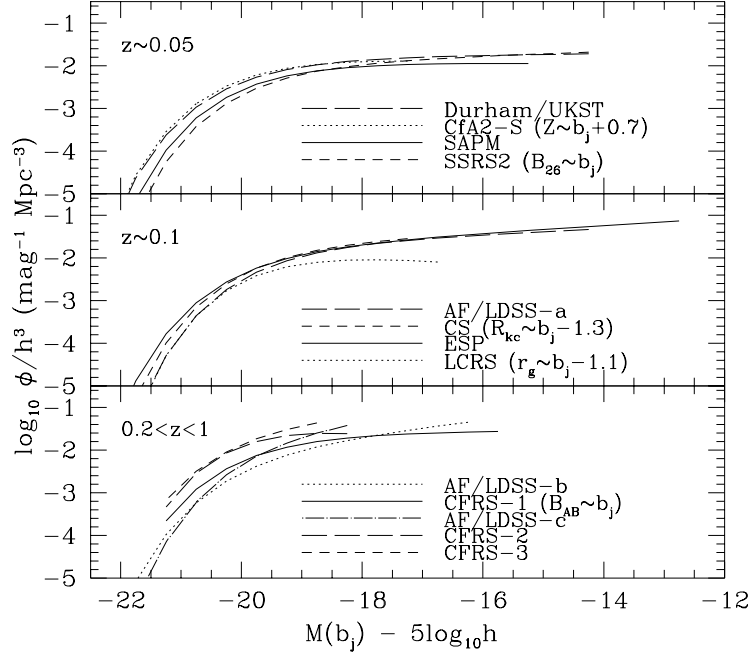


Fig. 2. — LFs with $\bar{z} \sim 0.05$ (top), with $\bar{z} \sim 0.1$ (middle), and with $\bar{z} > 0.2$ (see Table 2). The magnitude conversions are taken as quoted in the LF papers. The LFs are significantly different between each survey due to the diverse methodologies adopted in the selection of galaxies and in the measurements; it emphasizes that the quantification of the LF evolution is more securely understood within one single well-defined sample.

[23]). Knowledge of the shape of these local LFs is crucial for future distant LFs, to see how each class evolves, and which ones dominate the evolution at a certain cosmic epoch. Not discussed in this lecture are the K -selected redshift surveys (see [20], [10]); in this case *nearby* galaxies are selected on their mass even more than with a R - or I -selection.

6.2. Distant LFs

The selection of galaxies in the red pass-band allowed for the first time to probe the evolution of galaxies up to $z \sim 1$ (CFRS; see Fig. 3). This was followed by the larger CNOC2 survey which probes more finely the evolution for each individual galaxy type up to $z \sim 0.6$. In parallel the Autofib team collected all their B-selected surveys (DARS, AF-bright, AF-faint, BES, LDSS1, LDSS2), and also demonstrate evolution in the field population up to $z \sim 0.8$.

The present status is summarized below, but note that when I write 'compat-

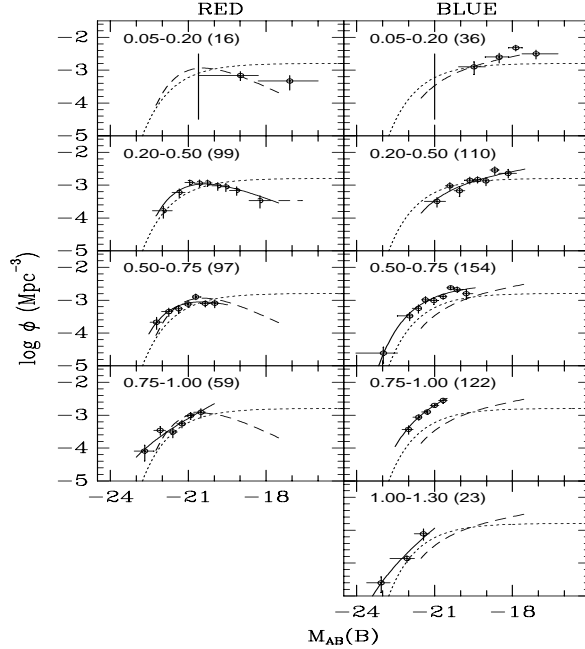


Fig. 3. — CFRS V_{max} estimates by $(V-I)$ color types at different cosmic epochs, see [32] for more details ($q_0 = 0.5, h = 0.5$). This survey demonstrated definitely the galaxy population evolution from $z \sim 1$ to today.

ible’, it does not mean that this is the only explanation. Indeed distinguishing between density and luminosity function requires further analyses than solely the LF studies. The main conclusions are:

- (a) The overall LFs at $\bar{z} < 0.5$ show a normalization similar to that found at $\bar{z} \sim 0.1-0.3$.
- (b) Early-type LF has a negative slope, and evolution is detected for galaxies at $M(B_{AB}) - 5 \log h < -20$ roughly, compatible with luminosity evolution, and modest or no density evolution.
- (c) Intermediate-type LF has a slope almost flat, and evolution is detected at about $M(B_{AB}) - 5 \log h < -20$, compatible with luminosity evolution.
- (d) Late-type LF has a steep slope, and evolution is detected in the steepening of the slope, compatible with modest luminosity evolution and strong density evolution.
- (f) The faint-end slope at $M(B_{AB}) - 5 \log h > -18$ is not yet observed at $z > 0.5$. The picture of this differential evolution will be quantified in detail in the near future with larger and deeper surveys, and several objective classification, and multi-color selection schemes. The availability of a large well-defined databases will precisely refine the evolution of each type of galaxy. For instance we would

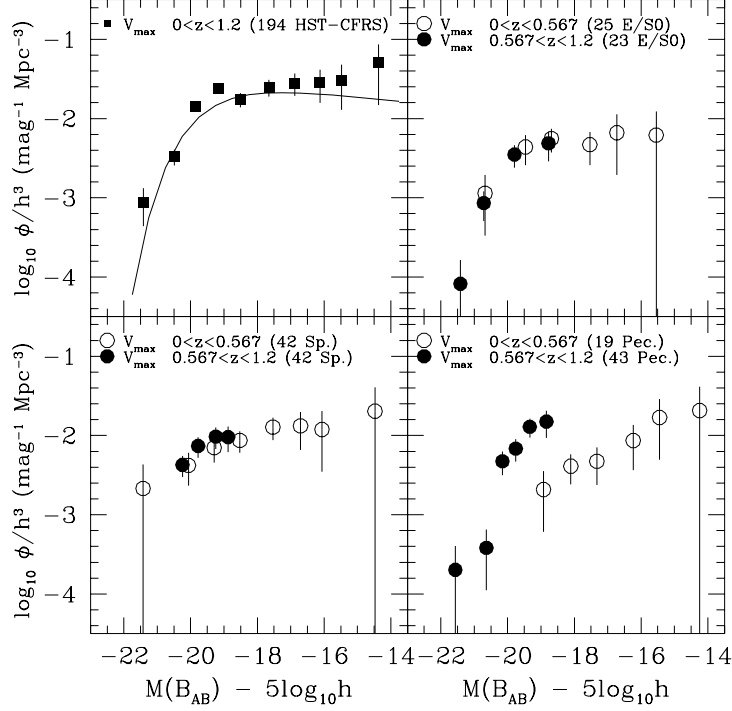


Fig. 4. — V_{max} estimates by HST eyeball morphological types for a sub-set of the CFRS galaxies. Top-left panel: V_{max} for the 194 HST/CFRS galaxies (dots) and the Schechter function fit of the whole CFRS (curve). V_{max} in the low (open dots) and high (filled dots) redshift range of the CFRS; for E/S0 (top-right), for spiral (bottom-left) and for peculiar (bottom-right) HST types. Bars are Poisson errors. ($q_0=0.5$)

like to: differentiate between number density evolution and evolution in clustering properties; to relate morphological type, spectral properties and environment; to better constrain the faint-end LF slope at all redshifts for each type of galaxies. Figure 4 illustrates the V_{max} estimates using HST eyeball morphological types as tabulated in [3]; we can see that the sample is barely large enough to test for *overall* LF evolution split by morphological types. However the estimates around L^* do agree within the uncertainties with the summary picture described above. The absence of bright irregulars at $z < 0.5$ is particularly noticeable; if they exist they would certainly be visible. This lack is expected since the L^* of local late-type galaxies is much fainter than the other types. The picture at higher redshifts is significantly different even allowing for possible misclassification, and is responsible for the strong evolution seen

in deep blue counts (see [3] for a detailed discussion). I note that significant discrepancies are likely to be found between different methods used to define or classify galaxies. The acquisition of several colors, and the development of objective classifications should be a great help to quantify the evolution of individual population (see e.g. lecture of Abraham for morphological classification, or [9] for spectral types).

With this caveat, these deep surveys have shown that the population which exhibits the strongest LF evolution is composed of galaxies with strong emission lines, blue colors, peculiar morphologies, and relatively small sizes. The LFs for remaining population evolves mildly or passively mainly at $L > L^*$. Their faint-end slope is close to flat, which indicates moderate or little star-formation activity. The difference in evolution for these two populations reflects many different processes in galaxy formation. Some of the massive systems formed at early epochs ($z \geq 2$), and then have a declining star formation rate giving the redder galaxies consistent with passive evolution, while other massive systems still exhibit star formation at recent epochs. Smaller systems that form later ($z \sim 1$) are seen during their early phase of intense star formation. Also smaller gas-rich systems may merge at any z ; a short starburst phase during the merger would contribute to the bright late-type galaxy LFs seen at $z > 0.5$, where both irregular morphologies and high star-formation rate are seen. A starburst during initial collapse, or during a merger has a very short timescale, and very quickly a stable phase is reached where the galaxy fades under passive evolution. Semi-analytical models and more recently N-body models which incorporate star-formation prescriptions include all of these processes, and are giving insights into which are the most dominant processes in the formation and evolution of galaxies and dark matter halos ([25], [1]). For a discussion on higher redshifts I refer to Dickinson's lecture, and to [50] for the Hubble Deep Field-North LFs at $1 < z < 4$. These LFs are preliminary since they are estimated with photometric redshifts and done on a single field of view.

7. CONCLUSION

Redshift survey analysis has been a crucial step forward in our understanding of galaxy evolution. We saw that all the steps in making a survey have their importance and each step needs to be carefully considered and well-defined. The luminosity functions are essential to quantify the evolution for different galaxy types. Larger and deeper surveys are necessary to precise the differential evolution of galaxy populations at all redshifts. Local surveys will give a refined and clearer picture at $z < 0.2$. Future surveys on 8m class telescopes equipped with new infrared capabilities will allow us to refine the evolution at $z < 1$, and systematic redshift surveys at $z \gg 1$ will be enabled. At the same time deep redshift surveys in other wavelengths (UV, far-IR, mm, radio) are also crucial to link the different emissivities of the galaxy populations, and to observe epochs of formation of the first stars. These will be crucial to differen-

tiate between models of galaxy formation and evolution.

ACKNOWLEDGMENTS I thanks J. Loveday and S. Maddox for their careful reading of the lecture. I thanks the organizers O. Le Fèvre and S. Charlot for this enjoyable school and for providing financial support.

References

- [1] Baugh C.M., Cole S., Frenk C.S. 1996, 283, 1361
- [2] Bingelli B., Sandage A., Tammann G.A., 1988, ARA&A, 26, 509
- [3] Brinchmann J. et al. ApJ, 499, 112, 1998
- [4] Bromley B.C., Press W.H., Lin H., Kirshner R.P. 1998, ApJ, 505, 25
- [5] Bruzual G., Charlot S. 1993, ApJ, 405, 538
- [6] Carlberg R.G., et al. 1998, Royal Society Discussion Meeting, March 1998, *Large Scale Structure in the Universe* (astro-ph/9805131)
- [7] Choloniewski J. 1987, MNRAS, 226, 273
- [8] Connolly A.J., Csabai I., Szalay A.S., Koo D.C., Kron R.G., Munn J.A. 1995, AJ, 110, 2655
- [9] Connolly A.J., Szalay A.S. 1999, ApJ, in press (astro-ph/9901300)
- [10] Cowie L.L., Songaila A., Hu E.M., Cohen J.G 1996, AJ, 112, 839
- [11] da Costa L.N., et al. 1994, ApJL, 424, 1
- [12] Davis M., Huchra J. 1982, ApJ, 254, 437
- [13] Eales S., 1993, ApJ, 404, 51
- [14] Ellis R.S. 1983, in *The origin and Evolution of galaxies*, eds. B.J.T. Jones, J.E. Jones, D. Reidel, Publishing Compagny, p. 255
- [15] Ellis R.S., Colless M., Broadhurst T., Heyl J., Glazebrook G. 1996, MNRAS, 280, 235
- [16] Efstathiou G., Ellis R.S., Peterson B.A. 1988, MNRAS, 232, 431
- [17] Felten J.E. 1976 AJ, 207, 700
- [18] Folkes S. 1997, PhD Thesis, University of Cambridge
- [19] Galaz G., de Lapparent V. 1998, in *Wide-field Surveys in Cosmology*, proceedings of XIV IAP meeting 1998
- [20] Gardner J.P., Sharples R.M., Frenck C.S., Carrasco B.E. 1997, ApJ, 480L
- [21] Geller M.J., Kurtz M.J., Wegner G., Thorstensen J.R., Fabricant D.G., Marzke R.O., Huchra J.P., Schild R.E., Falco E.E. 1997, AJ, 114, 2205
- [22] Heyl J., Colless M., Ellis R.S., Broadhurst T. 1997, MNRAS, 285, 613
- [23] Hogg D.W., Phinney E.S. 1997, ApJ, 488L, 95
- [24] Impey C., Bothun G. 1997, ARAA, 35, 267
- [25] Kaufmann G., Charlot S. 1998, MNRAS, in press (astro-ph/9802233)
- [26] Kirshner R.P., Oemler A., Schechter P.L. 1979, AJ, 84, 951
- [27] Kirshner R.P., Oemler A., Schechter P.L. Schectman S.A. 1983, AJ, 88, 1285
- [28] Kron R.G. 1980, ApJS, 43, 305
- [29] Kron R.G. 1982, Vistas in Astronomy, 26, 37

- [30] Lynden-Bell D. 1971, MNRAS, 155, 95
- [31] Lilly S.J., Le Fèvre O., Crampton D., Hammer F., Tresse L. 1995, ApJ, 455, 50
- [32] Lilly S.J., Tresse L., Hammer F., Crampton D., Le Fèvre O. 1995, ApJ, 455, 108
- [33] Lin H., Kirshner R.P., Shectman S.A., Landy S.D., Oemler A., Tucker D.L., Schechter P.L. 1996, ApJ, 464, 60
- [34] Lin H., et al. 1997 (astro-ph/9712244)
- [35] Loveday J., Peterson B.A., Efstathiou G., Maddox S.J. 1992, ApJ, 390, 338
- [36] Loveday J. 1996 MNRAS, 278, 1025
- [37] Loveday J. 1997 ApJ, 489, 29
- [38] Loveday J., Pier J. 1998 Proceedings of the 14th IAP meeting "Wide field surveys in cosmology", ed. Y. Mellier et al. (astro-ph/9809179)
- [39] Madau P., Pozzetti L., Dickinson M. 1998 ApJ, 498, 106
- [40] Maddox S.J., Sutherland W.J., Efstathiou G., Loveday J. 1990, MNRAS, 243, 692
- [41] Maddox S.J. 1998, in *Evolution of Large Scale Structure*, proceedings of MPA/ESO Conference Garching, August 1998, in press
- [42] Marzke R.O., Huchra J.P., Geller M.J. 1994, ApJ, 428, 43
- [43] Marzke R.O., da Costa L.N. 1997, AJ, 113, 185
- [44] Marzke R.O., da Costa L.N., Pellegrini P.S., Willmer N.A., Geller M.J. 1998, ApJ, 503, 617
- [45] Petrosian V. 1976, ApJ, 209, L1
- [46] Petrosian V. 1998, ApJ, 507, 1
- [47] McGaugh S.S. 1994, Nat, 367, 538
- [48] Ratcliffe, A., Shanks, T., Parker Q.A., Fong R. 1998, MNRAS, 293, 197
- [49] Sandage A., Tammann G.A., Yahil A. 1979, ApJ, 232, 352
- [50] Sawicky M.J., Lin H., Yee H.K.C. 1997 AJ, 113, 1
- [51] Schmidt M. 1968, ApJ, 151, 393
- [52] Sprayberry D., Impey C.D., Irwin M.J., Bothun G.D. 1997, ApJ, 482,104
- [53] Springel V., White S.M. 1998, MNRAS, 298, 143
- [54] Steidel C.C., Giavalisco M., Adelberger K.L., Pettini M., Dickinson M., Adelberger K.L. 1996, ApJL, 462, 7
- [55] Tresse L., Maddox S.J. 1998, ApJ, 495, 691
- [56] Turner E.L. 1979, ApJ, 231, 645
- [57] Willmer C.N.A. 1997, AJ, 114, 898
- [58] Zucca E., et al. 1997, AA, 326, 477